processes

MDPI

Article

Experimental and Simulation Study on the Direct Contact Condensation of Saturated Steam on Moving Droplets at Sub-Atmospheric Pressure

Yuanlin Jing [1,2], Yiping Wang [1] and Qunwu Huang [1,*]

[1] School of Chemical Engineering and Technology, Tianjin University, Tianjin 300072, China
[2] School of Energy and Chemical Engineering, Tianjin Renai College, Tianjin 301636, China
* Correspondence: huangqw@tju.edu.cn

Abstract: The recovery of low-temperature steam is of great significance to the effective utilization of energy. Direct contact condensation (DCC) technology is an effective heat recovery method with a low initial investment. An evaluation of the direct contact condensation heat transfer technology of water droplets and low-temperature saturated steam (at an absolute pressure of 7.3–19.9 kPa) was performed using both experimental and computational approaches. In the experiment, an experimental device based on the weighing method was set up, and the direct contact heat transfer process between droplets with a normalized diameter of less than 21.7 and saturated pure steam at 40–60 °C was experimentally investigated. The transient condensation efficiency and heat transfer coefficient were calculated by the real-time mass variation. The rapid condensation stage was classified to discuss the effects of initial droplet diameter, pressure, temperature, and mass flow rate on the heat transfer process. A two-dimensional model was developed using computational fluid dynamics techniques and verified by experimental results. The results indicated that when the normalized diameter of the droplet is less than two, 1.6 is the optimal value for DCC. For droplets with a normalized diameter greater than two, the optimal droplet temperature and mass flow rate are 15 °C and 10 g/s, respectively.

Keywords: direct contact condensation; droplets; saturated steam; heat transfer coefficient; numerical simulation

Citation: Jing, Y.; Wang, Y.; Huang, Q. Experimental and Simulation Study on the Direct Contact Condensation of Saturated Steam on Moving Droplets at Sub-Atmospheric Pressure. *Processes* **2023**, *11*, 1097. https://doi.org/10.3390/pr11041097

Academic Editor: Ireneusz Zbicinski

Received: 6 March 2023
Revised: 30 March 2023
Accepted: 31 March 2023
Published: 4 April 2023

1. Introduction

Direct contact condensation (DCC) heat transfer occurs when the vapor phase contacts a cooling surface or a fluid has a temperature below the vapor saturation temperature, and the vapor phase partially or completely condenses into the liquid phase [1]. The DCC process has many advantages, including a higher heat transfer coefficient, relatively simple equipment structure, and no metallic heat transfer surfaces that are prone to corrosion and fouling [2–4]. The DCC of steam on water droplets is a common phenomenon encountered in many industrial applications, particularly in the chemical and nuclear industries (such as degassing, direct contact condensers in thermal power plants, vacuum cooling, spray dehumidification, emergency core cooling, etc.) [5–7]. In most of the above applications, the subcooled liquid is sprayed into the saturated steam space through the nozzle, and its morphology generally changes from liquid sheets or jets to water droplets of various sizes [8]. The heat and mass transfer mechanism of the DCC of the steam on a single droplet is of fundamental importance for the design and optimization of a direct contact heat transfer exchanger.

When a cold droplet falls through the saturated vapor, the droplet size and average temperature change due to the phase transition [9]. Many theoretical and numerical studies have been carried out on the mechanism of droplet revolution. In the theoretical studies, a dimensionless temperature theoretical model has been developed based on the heat

transfer equation. Skelland and Wellek [10] established a theoretical correlation between the dimensionless temperature and Sherwood number for droplets with a Reynolds number between 400 and 3100 and a Sherwood number between 330 and 3600. They proposed that when the Reynolds number of a droplet is greater than 200, its oscillation increases the mass transfer rate. Rose [11] put forward a model for the oscillation of droplets, which considers that the droplets are composed of an inner part with uniform temperature and an outer layer with a thickness of δx. Ford [12] proposed an equation of droplet size change based on the pure heat conduction model. They assume that the droplet is a rigid sphere on which the steam condenses instantaneously, and the thermal resistance on the steam side is negligible. Pasamehmetoglu [13] modified Ford's dimensionless temperature equation by adding an empirical correction factor C to account for the turbulent and convective circulation within the droplet. Similarly, Ohba [14] obtained the temperature distribution of droplets by solving the conservation equation with the finite difference method considering the internal circulation of droplets. Some researchers theoretically analyzed the direct contact transmission process with emphasis on physics, involving droplet drag forces and flow field [15–17]. As for the numerical simulation, Zhen Yang [18] investigated the internal flow and heat transfer of the static droplet in steam flow, and the growth rate of droplets was found to increase with the steam flow rate. E.M. Bochkareva [19] modeled the influence of the droplet size and the initial parameters of the steam on the dynamics of depressurization during vapor condensation on the droplets. In the study by Annagrazia Orazzo [20], the effects of the Jakob number were analyzed to understand how condensation impacts the droplet heat flux and dynamics. Hengtao Ding [21] studied the direct contact condensation of saturated vapor to subcooled liquid spray, and the results indicated that the sheet region played the dominant role in the heat transfer process. Numerical simulation studies tend to focus on the hydrodynamics of static droplets or liquid layers and the characteristics of the external flow field in the steam environment [22–24]. However, there is no extensive knowledge about the rapid condensation process between a moving single droplet and low-temperature saturated steam without non-condensable gas, involving the formation and evolution of a single droplet and their changes in DCC [25].

Although some progress has been made in theoretical research, experiments are still necessary to validate the theoretical models and reveal the DCC heat and mass transfer mechanisms of a droplet in saturated steam. Lekic [12] experimentally studied the condensation of steam on water drops; the results showed that the approximate expression of the growth of the droplets based on the pure heat conduction model can describe the experimental results closely. Kulic [26] conducted an experiment on the condensation of air-steam mixtures on a single droplet; the results showed that the combined heat and mass transfer model incorporating partial internal mixing accurately predicted the temperature responses of the droplets. Hijikata [27] investigated the condensation of steam on droplets of refrigerant fluids; the results showed that the heat transfer coefficient is about ten times that of the rigid sphere and four or more times larger than the theoretical value due to the circulate motion in the spherical droplet. Celata and Takahashi [28,29] experimentally analyzed the direct contact condensation of saturated steam on spray droplets; the results showed that the droplet temperature is much higher than that obtained by the pure heat conduction model. It is considered that the oscillation of the droplet leads to internal turbulence and internal circulation. Pasamehmetogu's model predicts the temperature more accurately.

In the above experimental research, droplet diameter and temperature are the key parameters to evaluate the DCC heat and mass transfer characteristics. High-speed photography and pulsed laser holography were used to analyze the growth of drops [30]. The droplet diameter obtained by these two photography methods was equivalent to mean diameters rather than to true values, which makes errors inevitable. Additionally, the investigated time of contact was not sufficiently long due to the limited perspective of the camera equipment. Another parameter, the droplet temperature, was generally measured with a thermocouple and thermistor. Since the temperature of a single droplet is difficult to

measure accurately, the following two treatments were used: One was to collect multiple droplets in a small container and measure the average temperature [29]. Another method was to insert thermocouples or resistors directly into the flow field, in which case only the mixing temperature of the droplet and the surrounding steam could be measured, and the thermocouples interfered with the flow field [27]. Water splashing on the surface of the thermocouple assembly might affect the measured temperature signal. Other non-contact measurement methods, such as fluorescence displacement thermometry [31], can only obtain the average temperature of droplets within a period of time. As mentioned above, how to measure the key parameters more accurately and effectively is a significant topic in the study of the DCC of steam on droplets.

In addition to droplet evolution, it is necessary to analyze the influence of the important parameters (including droplet diameter, the initial droplet velocity/temperature, steam velocity, etc.) on the heat–mass transfer process. Some researchers indicated that the initial droplet diameter is the most important factor affecting heat transfer performance [32]. However, only a limited number of investigations have discussed the influence of droplet diameter parameters in detail. In past experiments on heat transfer between steam and droplets, the droplet size distribution was usually represented by statistical equations or by the mean diameters (Sauter mean diameter, volume mean diameter, or arithmetic mean diameter) [33–35]. It is considered that the mean diameter may only give macroscopic information about the behavior of the spray rather than clarifying the essence of the phenomenon. Therefore, it is necessary to study the influence mechanism of the single droplet parameters on the heat transfer process separately. Ford and Kulic [12,26] produced single drops ranging in size from 1.3 to 4 mm in diameter by using a hypodermic needle. They found that the bigger the droplet diameter, the slower its temperature changed. The increase in the temperature response time was attributed to the fact that the bigger droplets appeared to be experiencing more circulation. Mayinger [30] found that as droplet diameter decreased, heat transfer enhanced asymptotically and reached a maximum value. Celata [5] obtained liquid sprays with a uniform distribution of droplet diameters (mean diameters in the range of 0.3–2.8 mm). The experimental results showed that non-dimensional droplet temperature is a strongly decreasing function of the droplet diameter, especially for small droplets. For the droplets with large diameters, the temperature trend is always increasing in the investigated range. The behavior of droplets with very large diameters (e.g., 2.8 mm) was quite different and belonged to a different region. The behavior of each droplet and the effect of its parameters on heat transfer performance need to be further analyzed in a wider range of variables.

In this work, an experimental device based on the weighing method was established to study the rapid heat transfer process of the continuously falling single droplet in direct contact with saturated steam at sub-atmospheric pressure. Numerical simulation and its comparison with experimental results have been performed for more detailed results. The influence of initial droplet diameter and other parameters on DCC heat transfer performance is discussed in this article. The results of this study could provide a useful method to research the mechanism of direct contact heat transfer from steam on droplets, and give new reference to the design of the direct contact heat exchanger.

2. Experiment

2.1. Experimental Apparatus and Procedure

The droplet–steam direct contact condensation system mainly consists of a steam generation system, droplet generation system, direct contact condensation vessel (DCCV), and data acquisition system. The schematic diagram of the experimental setup is shown in Figure 1. Before the beginning of the experiments, the vacuum pump exhausted the non-condensable gas inside the whole experimental device, and the vacuum degree reached 0.099 MPa. The deionized water in the steam generator was heated by a cartridge heater. The heater was controlled by the temperature controller (AI-508A, UDIAN Co., Ltd., Xiamen, China), which was at 0.3% FS (full scale). A thermal resistance (±0.15 °C, 0.2% FS,

Pt100, Omega Co., Ltd., Shenzhen, China) was used to measure vapor temperature and was connected to the temperature control system. To achieve the goal of keeping a constant steam temperature, another low-power heater was installed in the tank. The steam was pumped into the container by the circulating pump (4A12A30R48B, Shenzhen Huachuang Co., Ltd., Shenzhen, China). Circulating steam served the purpose of preventing trace amounts of non-condensable gas from accumulating on the droplet surface. The droplet generation system was composed of a peristaltic pump, a liquid inlet valve, and a droplet outlet. When the steam reached a relatively steady state, droplets were injected into the negative pressure vessel with the aid of a high-precision peristaltic pump (LabN1, Shenchen Pump Co., Ltd., Shenzhen, China). The droplet temperature was controlled by a constant temperature water tank (DC-2006, Ningbo Scientz Biotechnology Co., Ltd., Ningbo, China). The flow rate and inlet tube diameter were precisely controlled to form single droplets with different initial diameters.

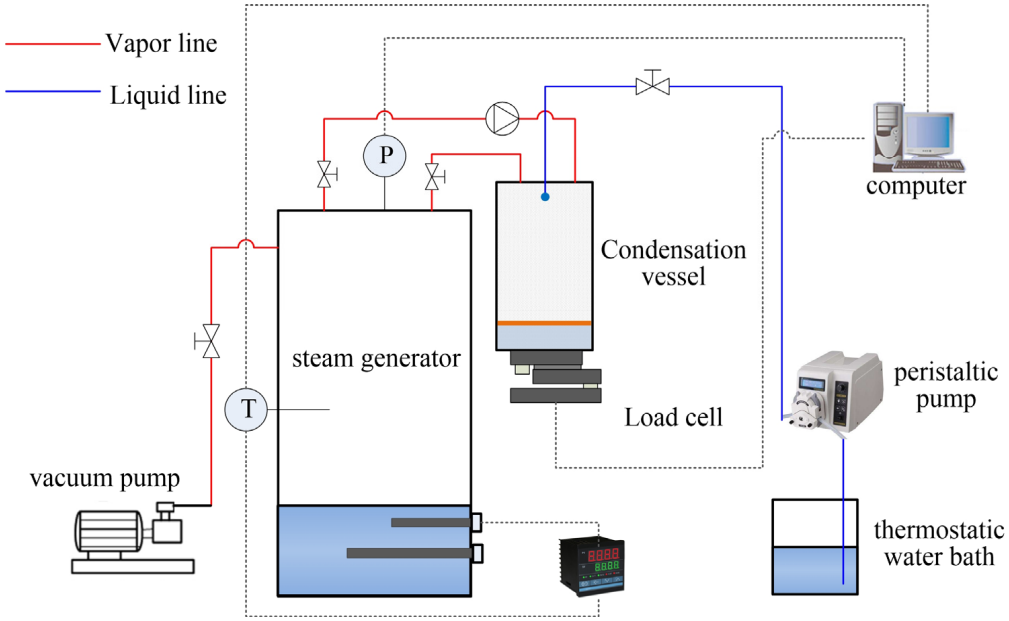

Figure 1. Scheme of experimental apparatus.

The DCCV is the core part of the system. DCCV is a cylindrical vacuum container, the wall of which is a double-layered vacuum structure. In order to reduce thermal loss, there was an insulating layer with a 5 mm thickness wrapping the vessel and pipes. The steam pipes were installed with a slight incline and the ambient temperature was higher than that of the steam, so as to prevent condensate from entering the container. There was a 3 mm oil seal on the liquid surface inside the container, which had extremely low thermal conductivity and good high-temperature stability to prevent steam from condensing on the condensate surface. When the steam and droplet were contacted directly, the mass transfer of the gas phase from the high-pressure phase to the low partial-pressure phase occurred, so that the gas phase condensed on the liquid surface. Therefore, the total amount of liquid accumulated in the container was greater than the actual liquid inflow, and the real-time weight difference was the condensation amount of steam, which could be measured by a high-precision weighing unit. The accuracy of this weighing method was 1% FS, which was explained in detail in the literature [36]. The range and uncertainty of each parameter during the test are shown in Table 1.

Table 1. Experimental parameters.

Parameter	Parameter Symbol	Value	Error
Vapor temperature, °C	T_s	40–60	±0.2%
Pressure, kPa	P	7.3–19.9	±0.2%
Droplet temperature, °C	T_i	10/15/20/25/30	±0.05%
Inlet water mass flow rate, g/s	m_{in}	1–20	±1%
Condensate mass flow rate, g/s	m_c	-	±1%
Droplet diameter, mm	d	-	±0.5%

2.2. Analysis Approach

2.2.1. Heat Transfer Rate

When saturated steam is in direct contact with droplets, the mass transfer direction is from steam to droplets due to the droplet temperature being lower than the steam temperature and the low fraction of non-condensable gases on the droplet surface, where condensation occurs on the droplet surface. In previous studies, the average condensation rate over a distance was obtained due to the limitation of the accuracy of the measurement method. In this study, the weighing method can accurately measure the transient change in the amount of condensate of steam, which is the difference between the total mass inside the vessel and the liquid inflow at any time interval. The transient heat transfer rate in any time interval from the contact of the droplet with the steam can thus be obtained. The heat transfer rate is calculated by the following equation [30]:

$$Q = m_c \gamma \tag{1}$$

where Q is the heat transfer rate, m_c is the mass flow rate of condensate, and γ is the steam latent heat.

2.2.2. The Transient Heat Transfer Coefficient

The transient heat transfer coefficient of DCC is calculated by means of the thermal balance equations as follows [30]:

$$h = \frac{Q}{A\Delta T} \tag{2}$$

$$\Delta T = T_s - T_d \tag{3}$$

where h, A, ΔT are the heat transfer coefficient, the sum of the surface areas of the droplets, and the temperature difference between the steam and the droplet surface. T_s and T_d are the temperatures of the steam and droplet. Since the steam is constantly circulating, the surface of the droplet is exposed to a constantly renewed constant temperature steam. The latent heat of condensation of the vapor is released and the droplet temperature increases. The droplet temperature is obtained according to the law of sensible heat balance [29]:

$$Q = m_{in} C_p (T_d - T_i) \tag{4}$$

where m_{in} is the mass flow rate of inlet water and C_p is the specific heat of the water.

During DCC, both the droplet radius and mass increase, so the heat transfer area also increases accordingly. The total heat transfer area is derived from the total droplet mass, with the additional condensate mass taken into account. The total mass and number of droplets can be expressed as:

$$m_L = m_{in} + m_c \tag{5}$$

$$n = \frac{6 m_L}{\pi d^3 \rho} \tag{6}$$

where m_L is the total mass of the droplets and n is the number of droplets. ρ is the water density and d is the droplet diameter. Then, the sum of the surface areas of all droplets at any time is the transient heat transfer area, which can be expressed as:

$$A = \frac{6m_L}{\pi d^3 \rho} \cdot \pi d^2 = \frac{6m_L}{d\rho} \tag{7}$$

Substitute Equations (1), (3), and (7) into Equation (2), then:

$$h = \frac{m_c \gamma}{A \cdot (T_s - T_d)} = \frac{\gamma d \rho m_c}{6(m_{in} + m_c)\left(T_s - \frac{m_c \gamma}{m_{in} C_p} - T_i\right)} \tag{8}$$

2.2.3. The Optimum Condensation Distance

The optimum condensation distance D_{opt} is one of the most important parameters to reflect heat transfer performance, which is defined as the necessary distance in which the saturated steam condensates rapidly. In this study, the optimum condensation distance is derived by an effective indirect method through condensation efficiency and mass change of droplets. The condensation efficiency, q, %, is defined as:

$$q = \frac{m_c}{m_{in}} = \frac{(m_L - m_{in})}{m_{in}}\% \tag{9}$$

2.3. Uncertainty Analysis

Experimental uncertainty is mainly the random error in the measurement process. Based on the measurement of different parameters, the uncertainties of heat transfer rate, heat transfer area, and heat transfer coefficient are calculated as:

$$\frac{\Delta Q}{Q} = \sqrt{\left(\frac{\Delta m_c}{m_c}\right)^2} = 1\% \tag{10}$$

$$\frac{\Delta A}{A} = \sqrt{\left(\frac{\Delta m_{in}}{m_{in}}\right)^2 + \left(\frac{\Delta m_c}{m_c}\right)^2 + \left(\frac{\Delta d}{d}\right)^2} = 1.23\% \tag{11}$$

$$\frac{\Delta h}{h} = \sqrt{\left(\frac{\Delta Q}{Q}\right)^2 + \left(\frac{\Delta A}{A}\right)^2 + \left(\frac{\Delta T}{T}\right)^2} = 1.03\% \tag{12}$$

From the above analysis, the computed maximum uncertainties of heat transfer rate, heat transfer area, and heat transfer coefficient are 1%, 1.23%, and 1.03%, respectively.

3. Simulation

The analysis was performed in the ANSYS-Fluent 2021 software. A 2D model was developed to predict the performance of direct contact condensation of low-temperature saturated water vapor on droplets. The length (y-coordinate) and width (x-coordinate) of the model were 200 and 70 mm, respectively. The inlet parameters that were considered were liquid mass flow rate and temperature. The "Volume of Fluid" (VOF) method was adopted in the simulation, and the Lee model was used to calculate interphase heat–mass transfer during the phase-change process. The simulated variables are summarized in Table 1.

3.1. Mesh and Boundary Conditions

The mesh geometry was generated by the commercial gridding software ICEM. The geometry of the model was meshed by quadrilaterals, which were more accurate and easier to process compared with the unstructured mesh. In order to elevate the precision and stability of the simulation, grids near boundaries were refined, and the mesh size of 86,718 quadrilateral cells was selected.

As shown in Figure 2, the wall of the vessel was set to be an adiabatic boundary with no heat flux, and the inner region was filled with negative pressure saturated steam. The inlets (droplet and vapor) were set as the velocity inlet and were set to several velocity values in the simulation. The outlet of vapor was set to pressure-outlet in ANSYS-Fluent.

The droplet and vapor temperatures were set to several values, and the vapor pressure was the saturated vapor pressure of the corresponding temperature.

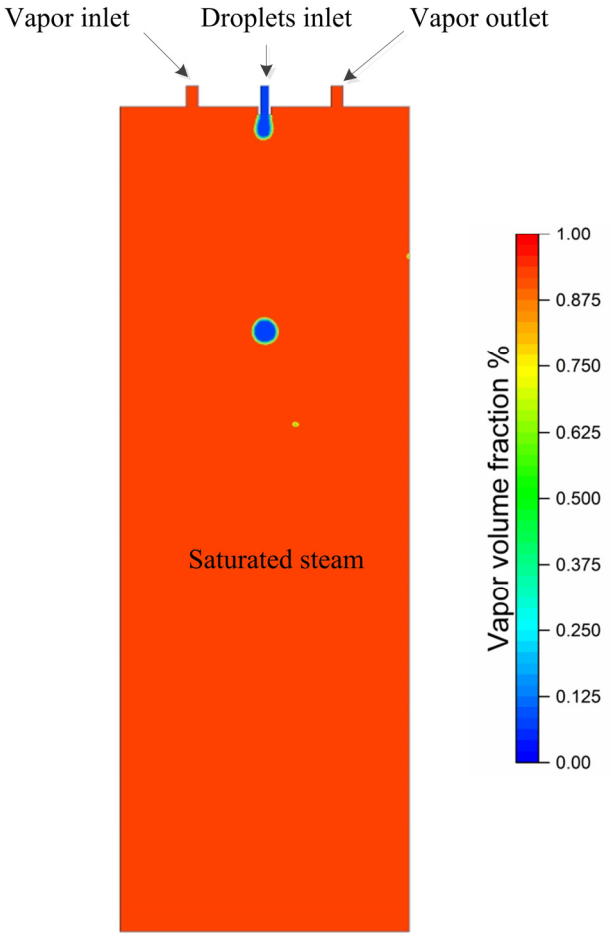

Figure 2. Volume fraction of vapor.

3.2. Numerical Methods

The transient solver and realizable K-Epsilon turbulence model were used in the simulation model. The VOF method was used, which introduced a volume fraction parameter for each cell ranging from 0 to 1. It reflects the volume ratio of phases in each grid cell to track the vapor–water interface. The theoretical model of phase transition in this simulation was the Lee model, which is divided into evaporation and condensation. The system determines whether the liquid phase transition has happened by the temperature on the grid. Phase transition happens when temperature deviates from saturation temperature. In this paper, because the temperature of saturated steam is higher than that of the droplet, the mass transfer direction is from steam to droplet; that is, the condensation phase transition happens. The theoretical model is expressed as follows [21]:

$$\text{If } T_d < T_s\text{: } \dot{m}_{vl} = coeff \cdot \alpha_v \rho_v \frac{(T_s - T_d)}{T_s} \tag{13}$$

where v denotes vapor phase, α_v denotes vapor volume fraction, ρ_v denotes vapor density, and $\dot{m}_{vl}$ denotes the rate of the mass transfer due to condensation, respectively.

The condensation frequency of this heat transfer model is determined by specific experimental conditions. In this paper, due to the minimal influence of non-condensable gas on the condensation mass transfer, the condensation frequency *Coeff* should be appropriately increased to match the experimental results with the numerical simulation results.

4. Results and Discussion

4.1. Evolution of the Droplet during Heat Transfer

The evolution of single droplets with different initial diameters during direct contact heat transfer with steam is shown in Figure 3. Figure 3A shows droplets with different initial diameters obtained by changing the inlet size and liquid flow rate. The initial diameter of the droplet is taken as its equivalent diameter just after leaving the inlet, which can be obtained from the two-dimensional area of the droplet. It can be seen from the figure that the initial diameter of the droplet is significantly small in some cases, which is due to the equilibrium between the gravity of the droplet and the surface tension at the moment of leaving the outlet, and a smaller surface tension corresponds to a smaller volume at this time. Figure 3B shows the trajectories of droplets with two different diameters. As for morphological changes, it can be found that the shape of the large droplet (d = 4.518 mm) changes most drastically when it just leaves the outlet, which is caused by its own velocity vector, and then gradually tends to be circular. In contrast, the morphology of the small droplet (d = 1.195 mm) did not change significantly, but the frequency was significantly accelerated, and it appeared as a string of beads after leaving the outlet.

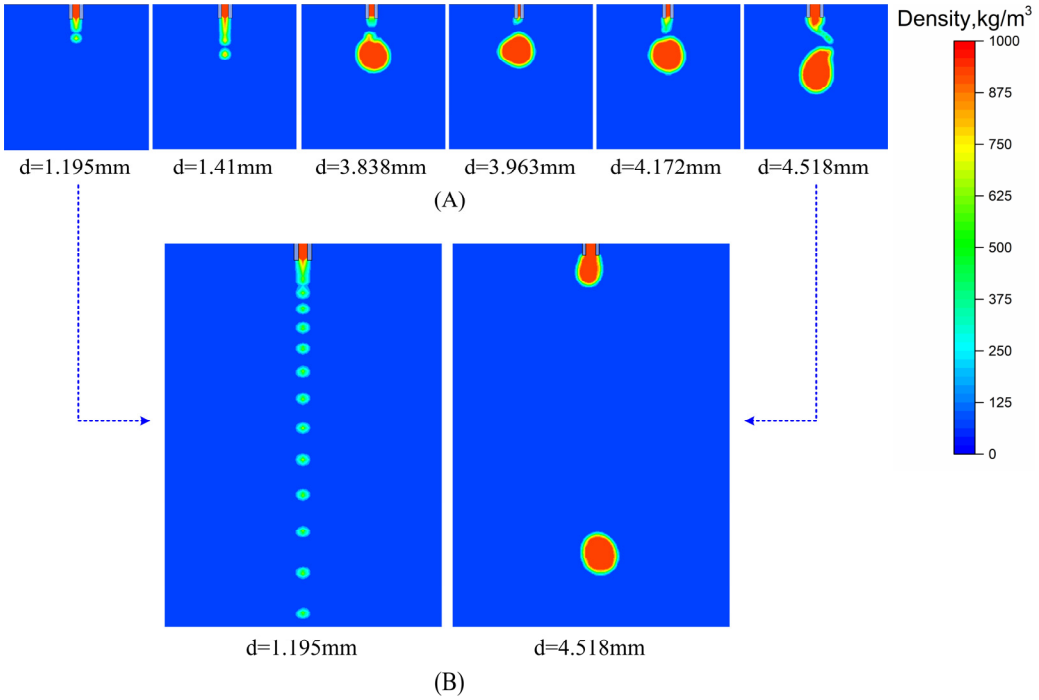

Figure 3. Evolution of a single droplet at different time steps: (**A**) formation of a single droplet with different initial diameters; (**B**) contour of the drop trajectory.

In order to further study the change of a single droplet during heat transfer, the density contour was established. The density contour of a single droplet with a time interval of 0.01 s during the falling process is shown in Figure 4. Due to the one-to-one correspondence between density and temperature under a certain pressure, the droplet is divided into three regions from inside to outside according to the density contour: low-temperature area, thermal boundary layer, and condensation boundary layer. The condensation efficiency can be calculated according to the area and proportion changes of each temperature zone, so as to analyze the heat transfer characteristics. It can be seen that the temperature of the large water droplets gradually increases from the outside to the inside during the falling process, the area of the thermal boundary layer does not change much, and there is still a large low-temperature area inside. The difference is that the number of isolines of the small droplets decreases rapidly after leaving the outlet; that is, the temperature gradient between the inside and outside decreases rapidly, and tends to reach temperature equilibrium after

a short period of time. It can be seen that the small droplet and the large droplet show different heat transfer characteristics. In the subsequent analysis, the effect of the initial diameter on the rapid condensation process is discussed according to whether the heat transfer equilibrium is rapidly approached.

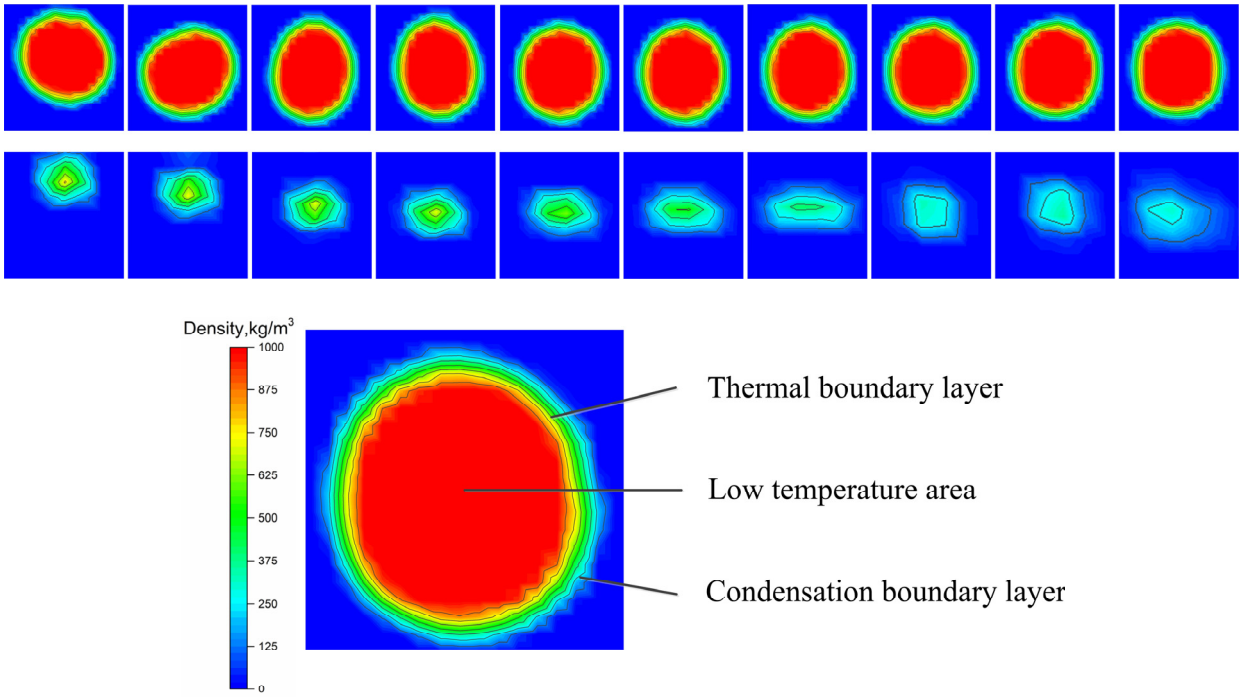

Figure 4. Density contour of a falling droplet.

4.2. Effect of Initial Diameter on the DCC Process

The condensation efficiency of the steam is represented as an index of heat transfer performance, which changes in the process of heat transfer. The droplet inlet position was set as the origin of the coordinates. The vertical downward directions and horizontal rightward were set as the positive directions on the *X* and *Y* axes. The condensation distance increases along the *x*-axis. The condensation efficiency along the *X* axe is illustrated in Figure 5.

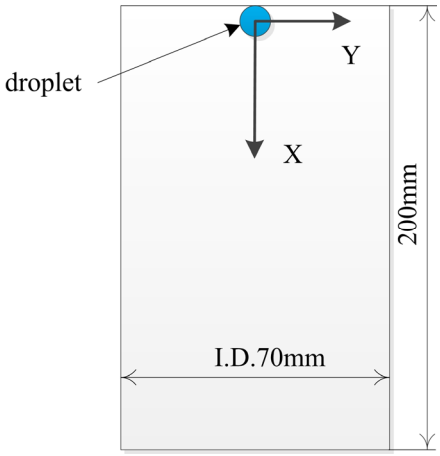

Figure 5. Test section.

The condensation efficiency of droplets with different diameters during heat transfer is shown in Figure 6. The simulated results are consistent with experimental results. Both experimental and simulation results show that when water droplets enter the steam,

the steam condenses rapidly and the condensation efficiency rises sharply. The rapid condensation stage is defined as the period where condensation efficiency increases rapidly. As the condensation distance increases, the condensation efficiency increases slowly. The optimum condensation distance (D_{opt}) and the maximum condensation efficiency (q_{max}) are determined according to the condensation efficiency. For the condensation process in which the fast condensation stage is not obvious, D_{opt} represents the distance required for q to change at the maximum velocity to the steady state value (maximum condensation efficiency in the slow condensation stage) at $x = 0$, and the corresponding condensation efficiency is q_{max}. As the initial diameter of the droplet increases, the D_{opt} increases and the q_{max} decreases.

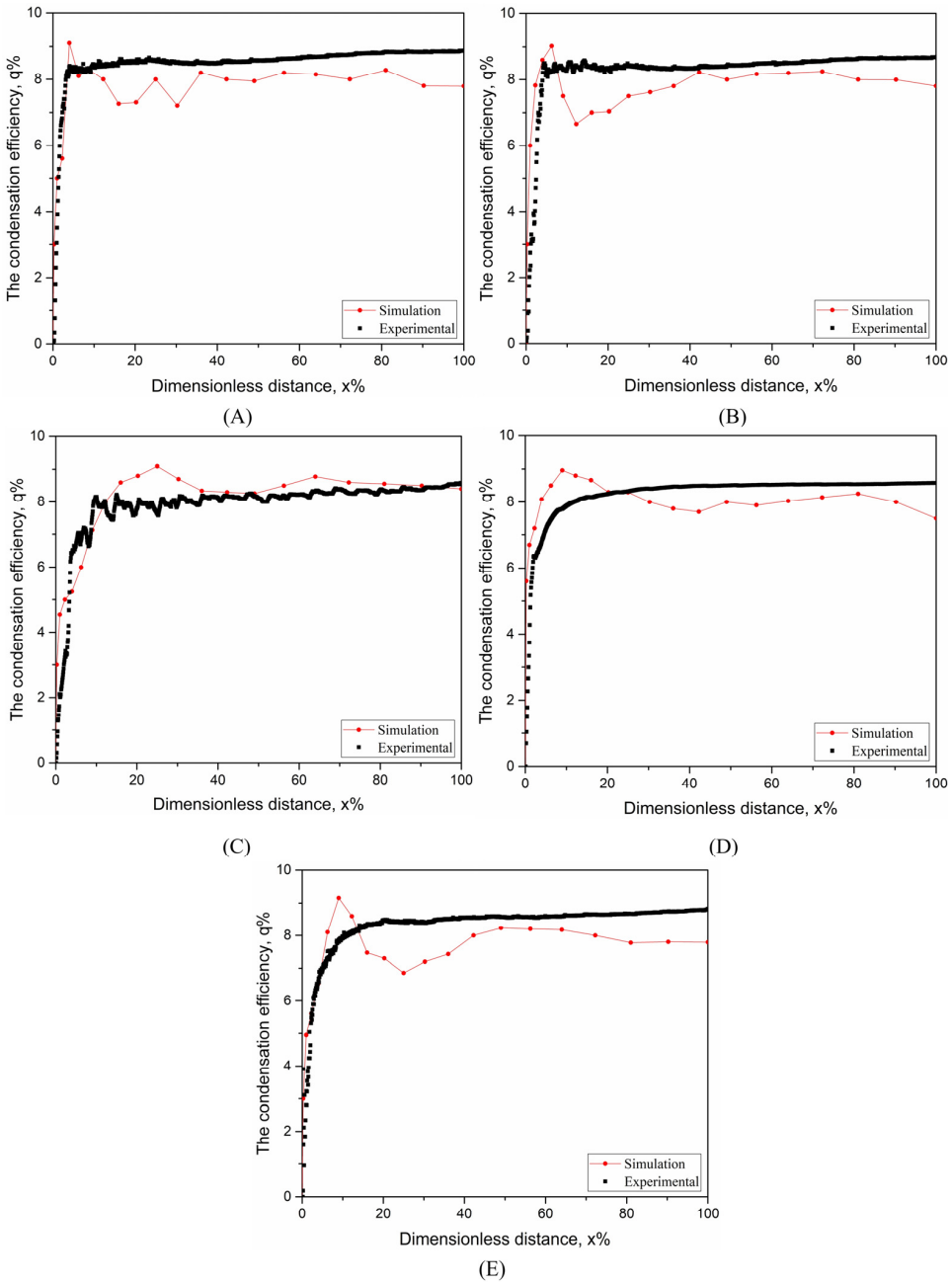

Figure 6. Experimental and simulation results of the condensation efficiency of droplets with initial diameters of (**A**) 1.195 mm, (**B**) 1.523 mm, (**C**) 4.01 mm, (**D**) 5.013 mm, and (**E**) 5.459 mm in direct contact with steam.

After the rapid condensation stage, the effect of droplet diameter on the condensation efficiency is almost negligible. In the slow condensation stage, the temperature of the droplet is still rising slowly because the complete heat transfer equilibrium is not reached, and the heat transfer mechanism becomes the heat conduction and the internal circulation convection within the droplet. The simulation results are lower than the experimental results because the droplet surface had a thermal interface layer with a temperature gradient, the droplet temperature gradually increased from the outside to the inside, and the low-temperature area gradually shrunk. In the experimental results, the condensation efficiency was obtained by using real-time mass variation. All steam condensing amounts were calculated into the condensing efficiency, including the mass of the condensing boundary layer, which was heating up. The fluctuation was caused by the uncertainty of sensors and transmission modules.

The maximum condensation efficiency and optimal condensation distance for droplets with different initial diameters and steam in the direct contact heat transfer process are summarized in Figure 7. The droplet diameter is normalized by the characteristic diameter, $d^* = \sigma / f\rho gr$, which represents the diameter scale of the droplets formed under different experimental conditions. The data in the figure show that different diameters have little effect on q_{max}. The q_{max} is much larger than that in the previous studies because of the use of precise load cells, which were capable of measuring real-time changes in condensate more accurately. Moreover, the non-condensable gas content is strictly controlled in this study, and a 1% increase in the non-condensed gas content can lead to a decrease in the condensation heat transfer coefficient of about 60%. However, it is still less than the heat transfer efficiency calculated based on the no thermal resistance theoretical model. With the increase in droplet diameter, the droplet volume had a higher increase relative to the droplet heat transfer surface. Therefore, the thermal balance of the droplet indicates that the increase in droplet diameter leads to a slightly decrease in condensation efficiency. It can also be seen from the figure that D_{opt} increased with the normalized diameter. The increasing rate of D_{opt} is significant when the normalized diameter is over two ($d/d^* > 2$). The D_{opt} for a droplet with a normalized diameter of 21.7 is approximately 10% higher than that of two. In contrast, for the normalized diameter under two ($d/d^* < 2$), the D_{opt} is less than 5% and the difference remains at a similar level. It shows that the droplets approach temperature equilibrium instantaneously after the rapid condensation process. Based on the different characteristics of droplets in the heat transfer process, small and large droplets should be discussed separately to further discuss the influence of other conditions on the DCC. In this article, the diameter is classified into two subgroups: LID ($d/d^* > 2$) and SID ($d/d^* < 2$).

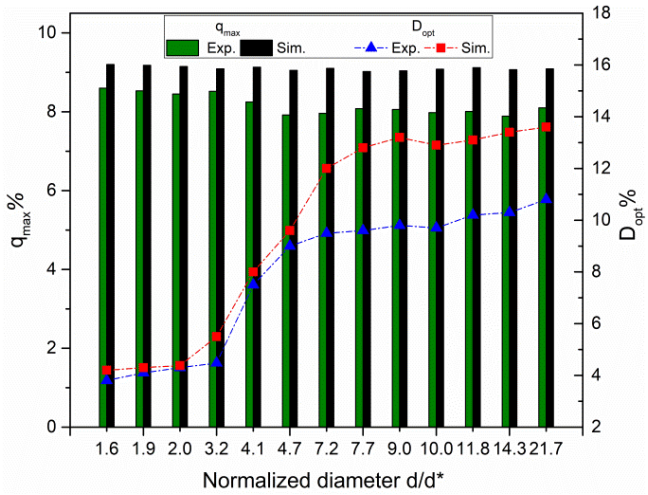

Figure 7. Effect of droplet initial diameter on q_{max} and D_{opt}.

4.3. Optimization

Optimizations for LID and SID were performed separately. The purpose of optimization is to select suitable inlet parameters to discuss the effect of condensation conditions on the DCC. For the LID, the rapid condensation stage in the direct contact condensation process is not obvious. The influence of pressure, temperature, and mass flow rate lead to the change of heat transfer characteristics. The factors involved in the condensation process become complex, so the trade-off of optimal conditions becomes more important. In order to optimize the condensation efficiency, the most preferable initial diameter was analyzed in the range of small droplets (SID). The optimization of the initial diameter was performed using the simulation model discussed above.

The optimum condensation distance and the breakup distance for SID are shown in Figure 8. It can be seen that when $d/d^* < 1$, the droplet has reached heat transfer equilibrium almost at the instant of leaving the outlet. When $d/d^* > 1$, the optimal condensation distance increases rapidly. D_{opt} gradually remains constant when d/d^* is between 1.6 and 2.0. For the droplet with $d/d^* < 1.6$, breakage occurs during the falling process; that is, the droplet breaks into several small droplets, and then breaks away from the vertical falling trajectory and rises in the airflow. This may be due to the fact that the small droplets are completely heated and atomized under the action of the steam flow at the same saturation pressure. The distance from the breakup point to the outlet decreases as the normalized diameter of the droplet decreases. The D_{opt} with $d/d^* = 1.6$ only increased by 3.2% compared with the droplet with $d/d^* = 0.4$. However, the droplet with $d/d^* > 1.6$ no longer broke up in the airflow. Therefore, it can be concluded that 1.6 is the optimal initial droplet diameter under this condensation condition.

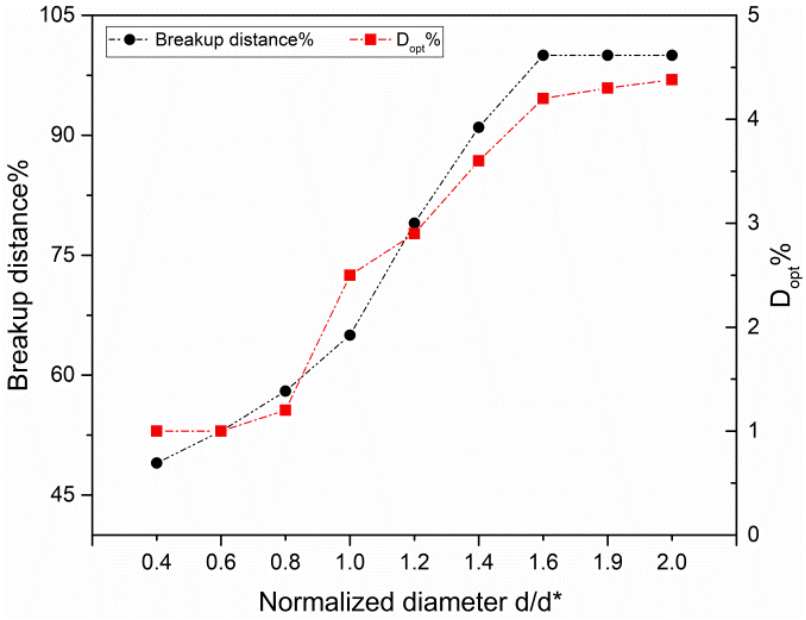

Figure 8. The optimum condensation distance and breakup distance for SID.

When the normalized diameter exceeds 2.0, the heat transfer equilibrium process is slow, and the optimal condensation distance is significantly longer. Therefore, it is necessary to optimize the condensation conditions for LID. The heat and mass transfer rate between vapor and liquid droplets under vacuum conditions is controlled by various parameters. According to previous studies, the influencing factors include pressure, mass flow rate, and temperature of gas–liquid phases. Figure 9 shows the influence of pressure, droplet temperature, and liquid mass flow rate on the DCC. As shown in Figure 9A, the D_{opt} of droplets with different initial diameters increases slightly with an increase in the absolute pressure, especially for small-diameter droplets. This indicates that the condensation rate of the vapor on the droplets increases with the increase in vacuum. This can be explained by

the following two facts. One is that as the vacuum increases, the steam dew point decreases and the temperature difference between steam and liquid decreases, which increases the driving force of heat transfer. The other is that under the vacuum condition, the steam density decreases and the steam velocity increases, which leads to the decrease in the heat and mass transfer resistance of the two vapor–liquid phases.

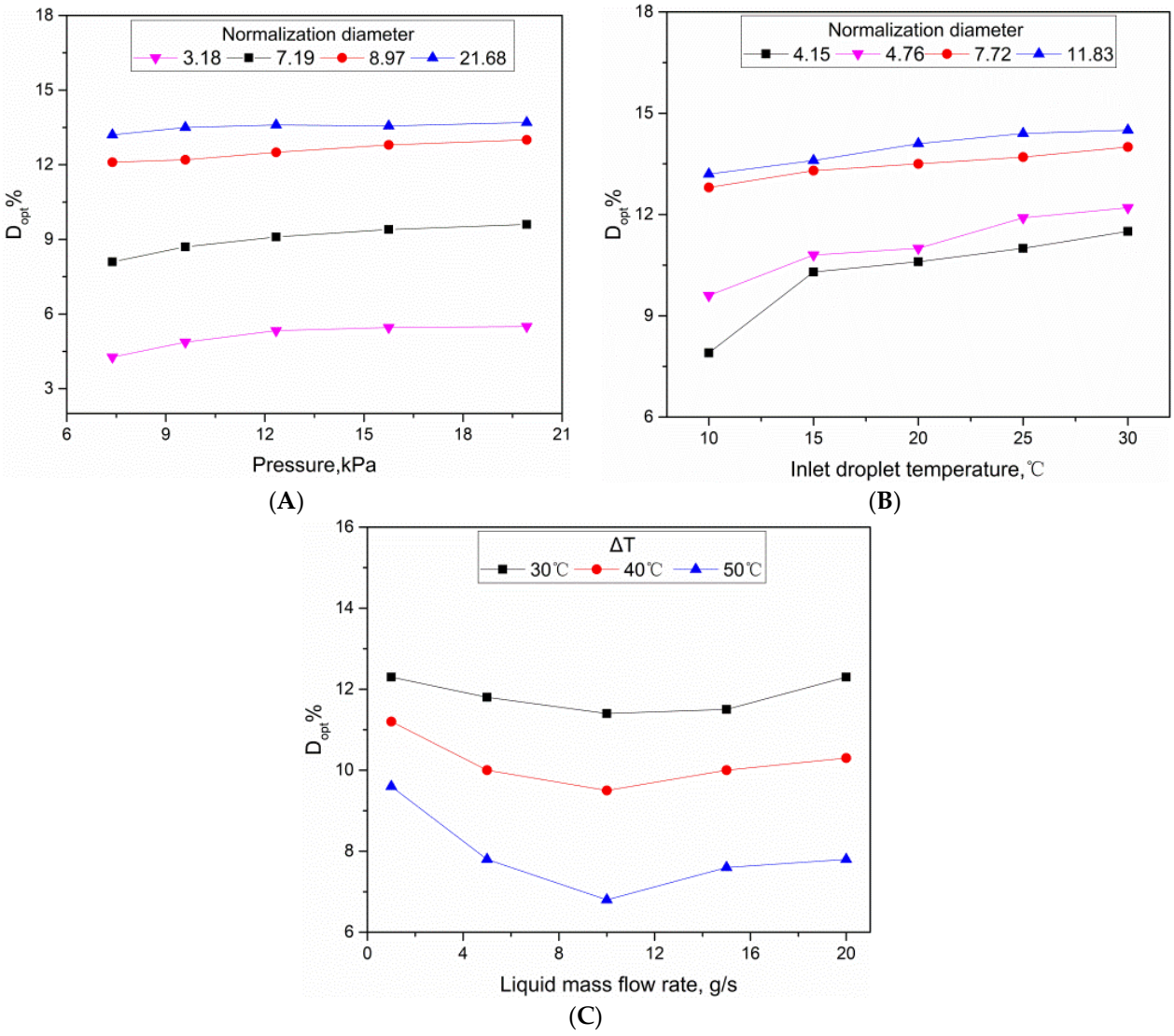

Figure 9. Influence of pressure (**A**), droplet temperature (**B**), and liquid mass flow rate (**C**) on the D_{opt}.

As shown in Figure 9B, the optimal heat transfer distance increases slightly with the increase in the droplet temperature. This is because when the inlet temperature increases, the driving force of the vapor–liquid two-phase temperature difference decreases, resulting in a decrease in the condensation rate. For smaller droplets, the effect of droplet temperature is greater than that of other conditions. This is because in the rapid condensation stage, the fresh surface area of the droplet exposed to the vapor is small, and the temperature difference between the gas–liquid phases becomes the main factor affecting the condensation efficiency. As shown in Figure 9C, the optimal condensation distance decreases with the increase in the liquid mass flow rate at a low-mass flow rate. It appears more obvious at high subcooling because the increase in liquid mass flow rate strengthens the liquid turbulence, and the enhancement of oscillation and internal turbulence increases the heat transfer efficiency. However, the optimal condensation distance increases when the mass flow rate of the liquid phase continues to increase. The reason is that the droplet is stretched

at the outlet to form a short liquid column, and the direct contact area between the fresh cold liquid surface and the steam is reduced, which reduces the heat transfer efficiency. On the other hand, a decrease in liquid temperature and an increase in flow rate will increase the energy consumption of the system.

4.4. Heat Transfer Analysis

The heat transfer coefficient is one of the vital indicators of direct contact heat transfer performance. The transient heat transfer coefficient of DCC along the dimensionless distance x% is shown in Figure 10 for different droplet diameters and a fixed value of the droplet velocity.

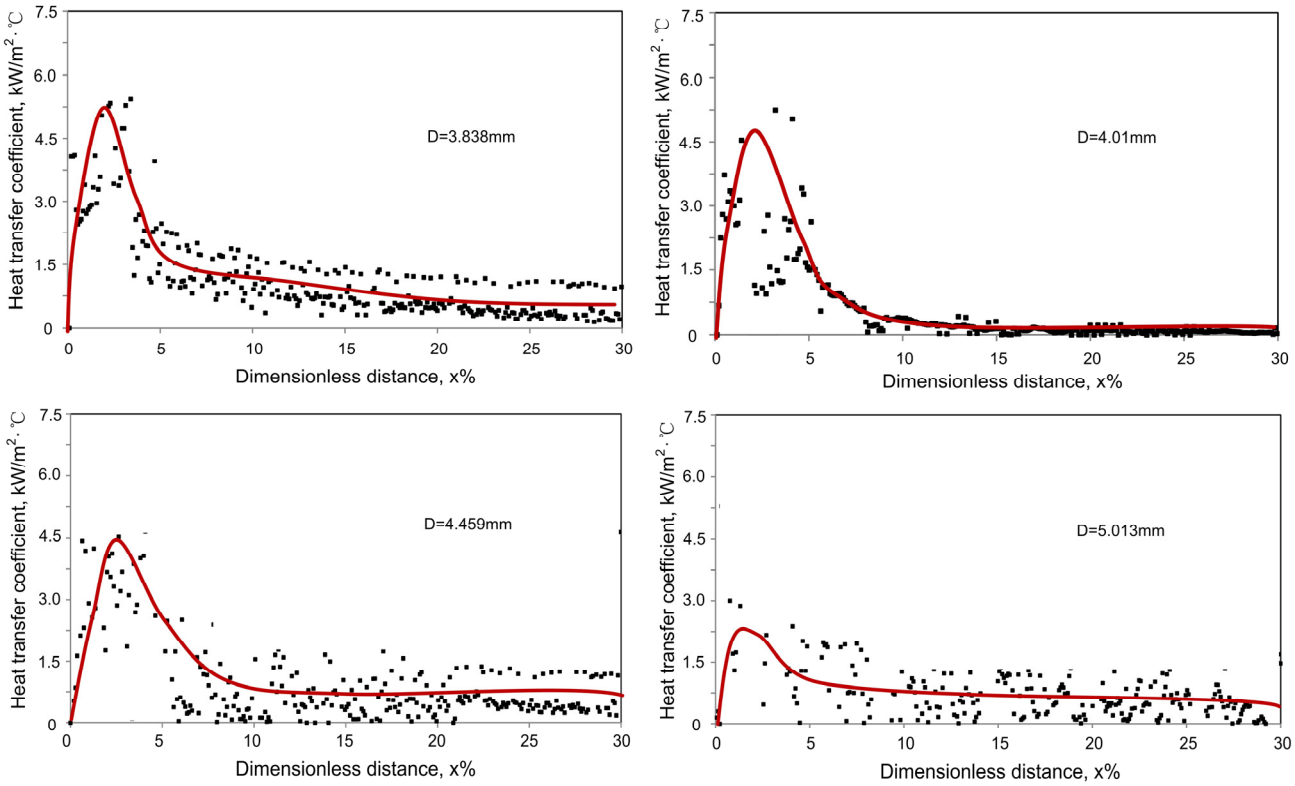

Figure 10. The transient heat transfer coefficient of a single droplet with different diameters.

As shown in Figure 10, within the dimensionless distance of less than 10%, the heat transfer coefficient increases sharply and then decreases gradually. In the rapid condensation phase, we observed a steep variation of $\partial h/\partial x^*$ as well as the maximum value of h, both of which exist within a dimensionless distance of less than 3%. When the dimensionless distance was greater than 15%, h almost remained stable. It is quite notable that h for the initial diameter of 3.838 mm reached 5.2 kW/(m^2·°C), which is almost twice as much as that of 5.013 mm. It also indicates that a smaller initial droplet diameter results in a larger heat transfer coefficient, which depends on reducing initial droplet diameter and enlarging heat transfer areas. Small droplets are rapidly generated at the inlet, causing the heat transfer areas to be renewed rapidly. The effect of the droplet's initial diameter on the transient heat transfer coefficient is almost negligible when the dimensionless distance is greater than 10%, and the transient heat transfer process is considered to have been basically completed.

5. Conclusions

The direct contact condensation heat transfer mechanism between droplet and steam is an important theoretical basis for the efficient recovery of low-temperature waste steam. Although thermocouples, photography, and other methods had been reported for data measurement obtaining real-time data in the whole range was still far away. Therefore, it is practical to propose an accurate and feasible real-time measurement approach. In addition, the heat transfer efficiency rises rapidly at a short distance from the droplet outlet, which is a rapid condensation stage. Although the macro information of this stage has been statistically studied, detailed conclusions are far from being drawn within a wider range of parameters. Therefore, it is of great significance to discuss the droplet–steam heat transfer phenomenon and the influencing factors in a more detailed way at this stage.

In this paper, the transient process of direct contact condensation of saturated steam on moving droplets at sub-atmospheric pressure was experimentally and numerically evaluated. A novel type of DCC system based on the weighing method was designed, which can be used to obtain real-time heat transfer data. The rapid condensation stage of DCC is discussed in detail, including the formation and evolution of droplets with different initial diameters and the effect of initial diameter on the heat transfer process. Further, the diameter is subdivided into subgroups to optimize the operation parameters. The simulated results are proven to be consistent with those achieved in the experiment. The experimental and simulation methods presented in this study, as well as the optimized operating conditions, can provide references for the application of direct contact condensation technology. The suggested droplet diameters should be considered in the DCC of saturated steam on moving droplets at sub-atmospheric pressure. The following conclusions are derived from the present work.

(1) Small droplets and large droplets show different heat transfer characteristics. With the increase in heat transfer distance, the area of the thermal boundary layer of large droplets is almost constant, and the area of the low-temperature region remains large over a long distance. In contrast, for small droplets, the internal and external temperatures quickly balance within a short distance from the outlet, and the rapid condensation stage is obvious.

(2) Normalized diameter d/d^* was used to evaluate the heat transfer behavior of the droplet, and the optimal condensation distance increased with the increase in normalized diameter. When d/d^* is greater than two, the increase rate of D_{opt} is significant. D_{opt} with a d/d^* of 21.7 was about 10% higher than D_{opt} with a d/d^* of 2. When is d/d^* is less than two, D_{opt} is less than 5%.

(3) For SID with $d/d^* < 2$, the dimensionless diameter of 1.6 is the optimal initial diameter under the condensation condition. The droplet with $d/d^* < 1.6$ has a cracking phenomenon when falling; that is, the droplet breaks into several small droplets, and then rises in the air flow after breaking away from the vertical falling track. This may be due to the small droplets being fully heated and atomizing under the action of steam flow under the same saturation pressure.

(4) For LID with $d/d^* > 2$, the optimal heat transfer distance slightly increases with the increase in pressure and droplet temperature, especially for the small droplet. When the droplet temperature is less than 15 °C, the condensation rate is significantly faster. When the mass flow rate of the liquid phase is small, the optimal condensation distance decreases with the increase in the mass flow rate, especially when the degree of subcooling is high. However, the further increase in the liquid mass flow rate leads to a decrease in condensation efficiency. The optimum set of parameters is an inlet fluid mass flow rate of 10 g/s and droplet temperature of 15 °C.

(5) For a droplet within the diameter range considered, the transient heat transfer coefficient is above 5.2 kW/(m^2 °C) in the rapid condensation stage. The maximum heat transfer coefficient decreases with the increase in the droplet initial diameter. The influence of diameter can be ignored when the dimensionless distance is greater than 10%.

Author Contributions: Conceptualization, Y.J., Q.H. and Y.W.; methodology, Y.J., Q.H. and Y.W.; software, Y.J.; validation, Y.J., Q.H. and Y.W.; data curation, Y.J., Q.H. and Y.W.; writing—original draft preparation, Y.J.; writing—review and editing, Q.H. and Y.W. All authors have read and agreed to the published version of the manuscript.

Funding: This research received no external funding.

Data Availability Statement: Not applicable.

Conflicts of Interest: The authors declare no conflict of interest.

Nomenclature

Q	heat release ratio of vapor, kW
m_c	mass flow rate of condensate, kg/s
m_{in}	mass flow rate of inlet water, kg/s
m_L	mass flow rate of droplets, kg/s
γ	latent heat of condensation, kJ/kg
h	heat transfer coefficient, kW/m^2 °C
ΔT	heat transfer difference, °C
T_s	saturated vapor temperature, °C
T_d	droplet temperature, °C
T_i	inlet temperature, °C
C_p	specific heat, kJ/(kg °C)
ρ	water density, kg/m^3
d	diameter of the droplet, m
d^*	characteristic diameter, m
Abbreviations	
DCC	direct contact condensation
DCCV	direct contact condensation vessel

References

1. Pasamehmetoglu, K.O.; Nelson, R.A. Transient direct-contact condensation on liquid droplets. In Proceedings of the National Heat Transfer Conference and Exhibition, Pittsburgh, PA, USA, 9 August 1987; Volume 3, pp. 7–10.
2. Apriyanti, V.; Adriansyah, W.; Abdurrachim; Pasek, A.D. A review of direct contact condensation of steam on water droplets. *AIP Conf. Proc.* **2018**, *1984*, 020035.
3. Weinberg, S. Heat transfer to low pressure sprays of water in steam atmosphere. *Proc. Inst. Mech.* **1953**, *1*, 240–258. [CrossRef]
4. Bron, G. Heat transmission by condensation of steam on a spray of water drops. *Proc. Gen. Discuss. Heat Transf.* **1951**, *1*, 49–52.
5. Celeta, G.P.; Cumo, M.; Annibale, F.D.; Farello, G.E. Direct contact condensation of steam on droplets. *Int. J. Multiph. Flow.* **1991**, *2*, 191–211. [CrossRef]
6. Lekic, A.; Ford, J.D. Direct contact condensation of vapour on a spray of subcooled liquid droplets. *Int. J. Heat Mass Transf.* **1980**, *23*, 1531–1537. [CrossRef]
7. Gumruk, S.; Aktas, M.K.; Kasap, F. Experimental investigation of spray dehumidification process in moist air. *Int. Commun. Heat Mass* **2018**, *97*, 163–171. [CrossRef]
8. Lee, S.Y.; Tankin, R.S. Study of liquid spray(water) in a non-condensable environment(air). *Int. J. Heat Mass Transf.* **1983**, *27*, 351–361. [CrossRef]
9. Lu, W.; Chen, Y. A study on direct contact condensation of a droplet falling through a saturated vapor atmosphere. *J. Chin. Inst. Eng.* **1980**, *3*, 95–103. [CrossRef]
10. Skelland, A.H.P.; Wellek, R.M. Resistance to mass transfer inside droplets. *AIChE J.* **1964**, *10*, 491–496. [CrossRef]
11. Rose, P.M.; Kintner, R.C. Mass transfer from large oscillating drops. *AIChE J.* **1966**, *12*, 531–534. [CrossRef]
12. Ford, J.D.; Lekic, A. Rate of growth of drops during condensation. *Int. J. Heat Mass Transf.* **1973**, *16*, 61–64. [CrossRef]
13. Pasamehmetoglu, K.O.; Nelson, R.A. *Direct-Contact Condensation on Liquid Droplets during Rapid Depressuri-Zation Part*; American Society of Mechanical Engineers: New York, NY, USA, 1987.
14. Ohba, K.; Kitada, H.; Nishiguchi, A. Direct Contact Condensation of Steam on a High Speed Spray Jet of Subcooled Water. *Proceeding Int. Cent. Heat Mass Transfer.* **1982**, *17*, 289–300.
15. Huang, L.J.; Ayyaswamy, P.S. Drag Coefficients Associated With a Moving Drop Experiencing Condensation. *J. Heat Transf. T Asme* **1987**, *109*, 1003–1006. [CrossRef]
16. Ayyaswamy, P.S. Direct-Contact Transfer Processes with Moving Liquid Droplets. *Adv. Heat Transf.* **1995**, *26*, 33–35.
17. Chung, J.N.; Ayyaswamy, P.S. Laminar condensation heat and mass transfer to a moving drop. *AIChE J.* **1981**, *27*, 372–377. [CrossRef]

18. Yang, Z.; Ma, X.; Duan, Y.; Chen, Y. Internal flow and heat transfer of a condensing water droplet in steam flow. *Chem. Eng. Sci.* **2013**, *94*, 54–59. [CrossRef]
19. Bochkareva, E.M.; Nemtsev, V.A.; Sorokin, V.V.; Terekhov, V.V.; Terekhov, V.I. Reduction in the Vapor Pressure in Condensation on Cold Droplets of a Liquid. *J. Eng. Phys. Thermophys.* **2016**, *89*, 553–558. [CrossRef]
20. Orazzo, A.; Tanguy, S. Direct numerical simulations of droplet condensation. *Int. J. Heat Mass Transf.* **2019**, *129*, 432–448. [CrossRef]
21. Ding, H.; Luo, Y.; Yuan, X. Numerical investigation of heat transfer in direct contact condensation of steam to subcooled water spray. *Chem. Eng. Process.* **2019**, *140*, 52–63. [CrossRef]
22. Ying, Z.; Yulong, L. Nonequilibrium molecular dynamics simulations of mass transfer on transient direct-contact condensation. *Int. J. Heat Mass Transf.* **2022**, *184*, 184. [CrossRef]
23. Boziuk, T.R.; Smith, M.K.; Glezer, A. Enhanced Two-Phase Heat Transfer by Direct-Contact Condensation Using Directional Acoustic Actuation. In Proceedings of the 25th International Workshop on Thermal Investigations of ICs and Systems (THERMINIC), Lecco, Italy, 25–27 September 2019.
24. Viswanath, V.; Peter, J.; Agarwal, D.K. Direct Contact Condensation of Subsonic, Inversely Buoyant Steam Jet in a stagnant Pool of Water, In Proceedings of the 8th International and 47th National Conference on Fluid Mechanics and Fluid Power, Guwahati, India, 9–11 December 2020.
25. Bureš, L.; Sato, Y. Direct numerical simulation of phase change in the presence of non-condensable gases. *Int. J. Heat Mass Transf.* **2020**, *151*, 119400. [CrossRef]
26. Kvlic, E.; Rhodes, E. Direct Contact Condensation from Air-steam Mixtures on a Single Droplet. *Can. J. Chem. Eng.* **1977**, *55*, 131–137.
27. Hijikata, K.; Mori, Y.; Kawaguchi, S. Direct contact condensation of vapor to falling cooled droplets. *Int. J. Heat Mass Transfer.* **1984**, *27*, 1631–1640. [CrossRef]
28. Celata, G.P.; Cumo, M.; Farello, G.E.; Focardi, G. A comprehensive analysis of direct contact condensation of saturated steam on subcooled liquid jets. *Int. J. Heat Mass Transf.* **1989**, *32*, 639–654. [CrossRef]
29. Takahashi, M.; Nayak, A.K.; Kitagawa, S.I.; Murakoso, H. Heat Transfer in Direct Contact Condensation of Steam to Subcooled Water Spray. *J. Heat Transfer.* **2001**, *123*, 703–711. [CrossRef]
30. Chavez, A.; Gebhard, P.; Mayinger, F. Measurement of Direct-Contact Condensation of Pure Saturated Vapour on an Injection Spray by Applying Pulsed Laser Holography. *Int. J. Heat Mass Transf.* **1993**, *35*, 691–702.
31. Lu, Q.Z.; Melton, L.A. Measurement of transient temperature field within a falling droplet. *AIAA J.* **2000**, *38*, 95–101. [CrossRef]
32. Luo, Q.; Ma, R.; Dong, B.; Li, W.; Gong, J. Simulation on heat and mass transfer for a subcooled droplet falling freely in saturated steam by the lattice Boltzmann method. *Int. J. Heat Mass Transf.* **2016**, *101*, 226–239. [CrossRef]
33. Lekic, A.; Bajramovic, R.; James, D.F. Droplet size distribution-an improved method for fitting experimental data. *Can. J. Chem. Eng.* **1976**, *54*, 399–402. [CrossRef]
34. Isachenko, V.P.; Kushnyrev, V.I. *Condensation Heat Transfer in Dispersed Liquid Spray*; Begel House Inc.: Danbury, CT, USA, 1974.
35. Mugele, R.A.; Evans, H.D. Droplet Size Distribution in Sprays. *Ind. Eng. Chem.* **1951**, *43*, 1317–1324. [CrossRef]
36. Jing, Y.; Guo, F.; Wang, Y.; Huang, Q. Influence of Piping on On-Line Continuous Weighing of Materials inside Process Equipment: Theoretical Analysis and Experimental Verification. *Appl. Sci.* **2021**, *11*, 5246. [CrossRef]